Robustness of interdependent hypergraphs: A bipartite network framework

Xingyu Pan and Jie Zhou [*]
School of Physics and Electronic Science, East China Normal University, Shanghai 200241, China

Yinzuo Zhou [†]
Alibaba Research Center for Complexity Sciences, Hangzhou Normal University, Hangzhou 311121, China

Stefano Boccaletti
CNR - Institute of Complex Systems, Via Madonna del Piano 10, Sesto Fiorentino, Florence, 50019, Italy; Universidad Rey Juan Carlos, Calle Tulipán s/n, Móstoles, Madrid, 28933, Spain; and Sino-Europe Complexity Science Center, School of Mathematics, North University of China, Shanxi, Taiyuan 030051, China

Ivan Bonamassa
Department of Network and Data Science, Central European University, Vienna 1100, Austria

(Received 28 September 2023; accepted 15 December 2023; published 12 January 2024)

In this paper, we develop a bipartite network framework to study the robustness of interdependent hypergraphs. From such a perspective, nodes and hyperedges of a hypergraph are equivalent to each other, a property that largely simplifies their mathematical treatment. We develop a general percolation theory based on this representation and apply it to study the robustness of interdependent hypergraphs against random damage, which we verify with numerical simulations. We analyze a variety of interacting patterns, from heterogeneous to correlated hyperstructures, and from full- to partial-dependency couplings between an arbitrary number of hypergraphs, and characterize their structural stability via their phase diagrams. Given its generality, we expect that our framework will provide useful insights for the development of more realistic venues to characterize cascading failures in interdependent higher-order systems.

DOI: 10.1103/PhysRevResearch.6.013049

I. INTRODUCTION

Natural systems often depend on one another to function. Modeling this feature can drastically change the robustness of coupled networks as compared to their isolated counterparts [1–4] since small damages get amplified, within and across scales, leading to macroscopic regime shifts [5]. Well-known examples pertinent to this finding often happen in manmade infrastructures such as blackouts in power grids [6–10], financial and ecological systems [11–13], and lie at the origin of extreme events such as transport congestion [14,15] or climate changes [16,17].

In the context of network theory, interdependent networks [18] provide a minimal theoretical [19–21] and experimental [22] framework to study these catastrophic events under realistic constraints. Thus far, models of interdependent systems focused mainly on pairwise dependency links between pairwise-coupled networks endowed with a broad variety of structural and functional patterns like partial dependencies [23], correlated structures [24–27], redundant dependencies [28], or multiple support or dependent interconnections [29–31], to name a few. However, a growing body of evidence shows that real-world systems may not be faithfully described by models based only on pairwise interactions, resulting in an increasing interest in higher-order network models [32–38]. In this light, a series of works have revealed essentially new outcomes induced from high-order interactions in a large variety of collective phenomena which are otherwise absent when only pairwise interactions are taken into account [37,39–46]. Paradigmatic examples are complex contagion processes [47–49] and ecosystems [50–53], where higher-order interactions yield new patterns in their structural and functional robustness or change the type of their phase transitions.

Motivated by these examples, models of interdependent higher-order networks have started attracting certain interest, raising mathematical and computational challenges to study their structural and dynamical properties [54–56]. In Ref. [57], in particular, a multiplex representation based on the factor graph of hypergraphs was put forward to analyze the properties of higher-order percolation on such structures under a variety of structural constraints. In this paper we study, instead, the percolation of a network of interdependent

[*]jzhou@phy.ecnu.edu.cn
[†]zhouyinzuo@163.com

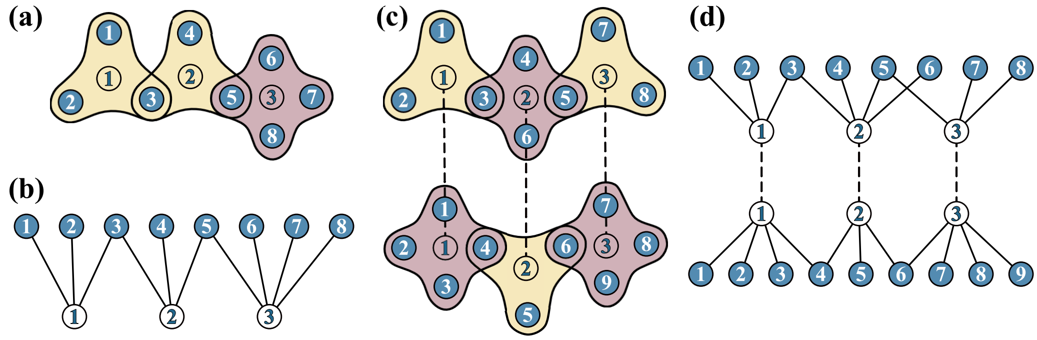

FIG. 1. Illustration of the bipartite representation of hypergraphs and interdependent hypergraphs. (a) A schematic plot of a hypergraph with three hyperedges, where the degree of hyperedge 1 (the left triangle-like shape in yellow) is three containing nodes 1, 2, and 3 (indexed in blue), the degree of hyperedge 2 (the middle one in yellow) is three containing nodes 3, 4, and 5, and the degree of hyperedge 3 (the right one in lilac) is four. (b) The bipartite network representation of the hypergraph in (a) where nodes and hyperedges are indexed in the same way. For this hypergraph $\mathcal{G}$, the number of nodes is $|\mathcal{N}^\top| = 8$, the number of hyperedges is $|\mathcal{N}^\perp| = 3$, and the number of node-hyperedge connections is $|\mathcal{E}| = 10$. (c) A schematic plot of two interdependent hypergraphs, where dashed lines connect the pairs of hyperedges in the two hypergraphs that are interdependent. (d) The bipartite network representation of the interdependent hypergraphs shown in (c).

hypergraphs (IHs) by relying on a bipartite network representation [58], where nodes and hyperedges are represented by two separated sets of topological objects and if a node is incident to a hyperedge then a bipartite link connects the node to the hyperedge. This representation produces an incidence matrix which enables us to fully and concisely characterize the robustness of interdependent hypergraphs by a suitable generalization of the generating function formalism [59]. We show that our bipartite framework can be conveniently applied to delicate scenarios, including correlated IHs, IHs composed by an arbitrary number of layers, and IHs with partial dependency couplings, whose analytical predictions are validated against numerical simulations.

The paper is organized as follows. In Sec. II we introduce the bipartite network representation to model a single hypergraph. Section III applies the bipartite model to hyperedge-IHs and a percolation theory is developed to analyze their robustness under cascading failures. Section IV contains the general case where interdependent hyperedges are correlated according to the order of the interaction they model (e.g., order 2 for pairwise links, order 3 for triples, n for n-tuples, and so forth). Section V describes the case where IHs are composed of an arbitrary number of hypergraphs, and Sec. VI extends the latter to the case of partial IHs where only a fraction of hyperedges in one layer are dependent on those in other ones. We present our conclusions in Sec. VII.

II. BIPARTITE NETWORK REPRESENTATION

In the bipartite network representation, nodes and hyperedges of a hypergraph are separated into two distinct sets, denoted as $\mathcal{N}^\top$ and $\mathcal{N}^\perp$, respectively. When a node is incidental to a hyperedge, a link is generated connecting the node and the hyperedge, which is regarded as a node-hyperedge connection. Elements in the same set do not connect directly and their relations can be read from the node-hyperedge connections [see Fig. 1(b) for an illustrative example]. By collecting all the node-hyperedge connections into the set $\mathcal{E}$, we obtain the full structural information of a hypergraph $\mathcal{G} = (\mathcal{N}^\top, \mathcal{N}^\perp, \mathcal{E})$, where the notation "$\top$" will be hereafter adopted to denote observables related to nodes and "$\perp$" for hyperedges. One can see that the number of links attaching to a node—say, k—which is defined as the degree of the node tells the number of hyperedges incident to it. Analogously, the number of links attaching to a hyperedge—say, m—denotes how many nodes it involves, which we referred to as the degree of this hyperedge. Accordingly, relevant degree distributions of the two sets are defined as $P^\top(k)$ and $P^\perp(m)$, respectively.

Within the bipartite network framework, the percolation behaviors of a hypergraph can be studied by generalizing the self-consistent arguments developed for the computation of the giant connected component (GCC) in single networks [59]. To do so, we suppose that a hypergraph is initially damaged by losing $1 - p^\top$ fraction of nodes and $1 - p^\perp$ fraction of hyperedges. Then, we define $S^{\top\prime}$ ($S^{\perp\prime}$) as the probability that a node (hyperedge) reached by a node-hyperedge connection belongs to the giant component of the hypergraph. For a node of degree k (incident to k hyperedges) that is not initially damaged and meanwhile reached by a hyperedge (through a node-hyperedge connection), the probability it belongs to the GCC equals the probability that at least one of the remaining $k-1$ hyperedges incident to this node belongs to the GCC, which gives $1 - (1 - S^{\perp\prime})^{k-1}$. Summing over all degree classes k and noting that the probability of a degree k node reached by a hyperedge through a node-hyperedge connection is proportional to its degree k, we have

$$S^{\top\prime} = p^\top\left[1 - \sum_k \frac{P^\top(k)k}{\langle k\rangle}(1 - S^{\perp\prime})^{k-1}\right]. \tag{1}$$

The same reasoning gives

$$S^{\perp\prime} = p^\perp\left[1 - \sum_m \frac{P^\perp(m)m}{\langle m\rangle}(1 - S^{\top\prime})^{m-1}\right]. \tag{2}$$

The observables $S^{\top\prime}$ and $S^{\perp\prime}$ are obtained by solving the self-consistent Eqs. (1) and (2), in terms of which the fraction of nodes and hyperedges that are contained in the GCC,

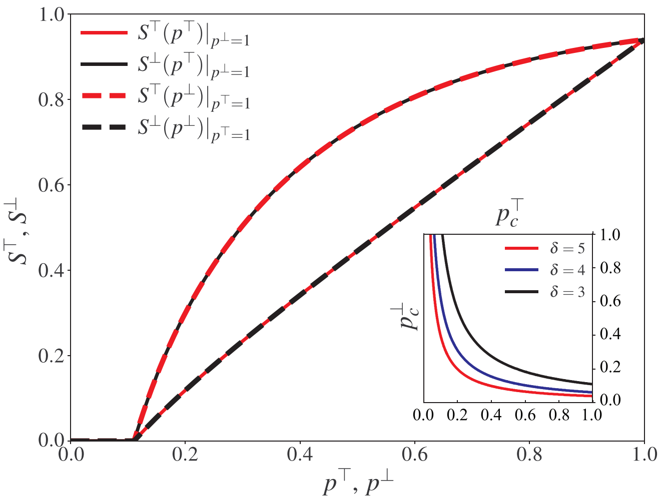

FIG. 2. Hypergraph percolation. Behaviors of $S^\top$ and $S^\perp$ as functions of $p^\top$ and $p^\perp$ for a single hypergraph. There are four situations: $S^\top(p^\top)|_{p^\perp=1}$ (red solid curve), $S^\perp(p^\top)|_{p^\perp=1}$ (black solid curve), $S^\top(p^\perp)|_{p^\top=1}$ (red dashed curve), and $S^\perp(p^\perp)|_{p^\top=1}$ (black dashed curve). The behaviors of $S^\top(p^\perp)|_{p^\top=1}$ and $S^\perp(p^\perp)|_{p^\top=1}$ and the behaviors of $S^\perp(p^\top)|_{p^\perp=1}$ and $S^\top(p^\perp)|_{p^\top=1}$ completely overlap, respectively. In this hypergraph, $P^\top(k)$ and $P^\perp(m)$ both follow Poisson distribution with their average $\langle k\rangle = \langle m\rangle = \delta = 3$. The inset shows the behaviors of the critical points $p_c^\top$ and $p_c^\perp$ on the $(p^\top, p^\perp)$ plane for the cases $\langle k\rangle = \langle m\rangle = \delta = 3, 4, 5$, respectively. According to Eq. (4), these curves give inversely proportional functions.

respectively $S^\top$ and $S^\perp$, can be evaluated via

$$S^\top = p^\top\left[1 - \sum_k P^\top(k)(1 - S^{\perp\prime})^k\right],$$
$$S^\perp = p^\perp\left[1 - \sum_m P^\perp(m)(1 - S^{\top\prime})^m\right]. \tag{3}$$

Equations (1) and (2) highlight the equivalent role, from the bipartite network perspective, played by site nodes and hyperedge nodes in the study of site-bond percolation in random hypergraphs. Moreover, they enable us to readily and unambiguously apply in the hypergraph realm the probabilistic methods underlying the generating function approach in pairwise graphs (see Appendix A).

Figure 2 shows the behaviors of $S^\top$ (red solid curve) and $S^\perp$ (black solid curve) with the growing of $p^\top$, where $p^\perp$ is set to be 1. For the convenience of comparison, in this hypergraph the degree distribution $P^\top(k)$ and the size distribution $P^\perp(m)$ both follow Poisson distribution with the same average value such that $\langle k\rangle = \langle m\rangle = \delta$. We observe a continuous phase transition at a critical point $p_c^\top$. When $p^\top > p_c^\top$, $S^\top$ grows almost linearly with the growth of $p^\top$. This observation implies that, above the critical point $p_c^\perp$, nodes that survived from the initial damage will be included in the GCC with a nearly constant ratio. Besides, since the initial damage does not directly act on hyperedges ($p^\perp = 1$), the extent in the loss of hyperedge $\perp$ is smaller than that of nodes $\top$, resulting in a greater score of $S^\perp(p^\top)|_{p^\perp=1}$ as compared to $S^\top(p^\top)|_{p^\perp=1}$. The dashed curves in Fig. 2 show the behaviors of $S^\top$ and $S^\perp$ in the converse situation where $p^\perp$ grows with $p^\top$ being set to be 1. We see that the curves of $S^\top(p^\perp)|_{p^\top=1}$ and $S^\perp(p^\perp)|_{p^\top=1}$ perfectly overlap the curves of $S^\perp(p^\top)|_{p^\perp=1}$ and $S^\top(p^\top)|_{p^\perp=1}$, respectively. This result manifests the equivalent roles of nodes and hyperedges in a hypergraph, where the impact of deleting a fraction of nodes on the nodes and hyperedges is equivalent to the impact of deleting a fraction of hyperedges on the hyperedges and nodes.

The critical points $p^\top = p_c^\top$ and $p^\perp = p_c^\perp$, where the hypergraph transits from non-percolating phase to percolating phase, could be evaluated by Eqs. (1) and (2) (details are provided in Appendix A). The expressions, Eqs. (1) and (2), give a reciprocal relation between $p_c^\top$ and $p_c^\perp$,

$$p_c^\top p_c^\perp = \left[\frac{\langle k(k-1)\rangle}{\langle k\rangle}\frac{\langle m(m-1)\rangle}{\langle m\rangle}\right]^{-1}, \tag{4}$$

which is consistent with what is found in Ref. [57]. The relation between $p_c^\top$ and $p_c^\perp$ on the condition $\langle k\rangle = \langle m\rangle = \delta$ is shown in the inset of Fig. 2, where it can be seen that large values of δ yield smaller values of the critical points, indicating a stronger robustness of the system to random failures.

III. INTERDEPENDENT HYPERGRAPHS

Consider now two hypergraphs, $\mathcal{G}_1 = (\mathcal{N}_1^\top, \mathcal{N}_1^\perp, \mathcal{E}_1)$ with degree distributions $P_1^\top(k)$ and $P_1^\perp(m)$ and $\mathcal{G}_2 = (\mathcal{N}_2^\top, \mathcal{N}_2^\perp, \mathcal{E}_2)$ with degree distributions $P_2^\top(l)$ and $P_2^\perp(n)$, whose hyperedges are interdependent in a one-to-one fashion [Fig. 1(d)]. The mutual percolating component of an IH requires not only that the nodes and hyperedges belong to the GCC of their own hypergraph but that the dependent nodes and hyperedges in the other hypergraph should belong to the GCC of their own hypergraph. This triggers a cascade of failures of nodes and hyperedges, whose back-and-forth propagation within and between layers of the interdependent hypergraph continues until no more elements are removed. We refer to the remaining component as the hypergraph mutually connected giant component (HMCGC). Since nodes and hyperedges are on an equal footing in the bipartite network representation, studying hyperedge-interdependent hypergraphs or node-interdependent ones are equivalent problems. In this paper, without losing generality, we consider the hyperedge-interdependency case, so that if a hyperedge (elements in $\mathcal{N}_1^\perp$ or $\mathcal{N}_2^\perp$) belongs to HMCGC, this hyperedge and the hyperedge dependent on it must belong to the GCC of their own hypergraphs, respectively, while nodes (elements in $\mathcal{N}_1^\top$ or $\mathcal{N}_2^\top$) in these hypergraphs are free from such constraint. We start, then, by studying the case where two hypergraphs are fully interdependent on each other, i.e., such that all the hyperedges in one hypergraph are dependent on those in the other hypergraph. This condition immediately implies $|\mathcal{N}_1^\perp| = |\mathcal{N}_2^\perp|$ under one-to-one correspondence.

Let $S_1^{\top\prime}$ ($S_1^{\perp\prime}$) be the probability that a node (hyperedge) of $\mathcal{G}_1$ reached by a randomly chosen node-hyperedge connection in $\mathcal{G}_1$ belongs to the HMCGC, and $S_2^{\top\prime}$ ($S_2^{\perp\prime}$) are defined similarly. Supposing initially that $\mathcal{G}_1$ is damaged by losing

$1 - p^{\top}$ fraction of nodes and $1 - p^{\perp}$ fraction of hyperedges, we have

$$S_1^{\top\prime} = p^{\top}\left[1 - \sum_k \frac{P_1^{\top}(k)k}{\langle k\rangle}(1 - S_1^{\perp\prime})^{k-1}\right], \tag{5a}$$

$$S_1^{\perp\prime} = p^{\perp}\left[1 - \sum_m \frac{P_1^{\perp}(m)m}{\langle m\rangle}(1 - S_1^{\top\prime})^{m-1}\right] \times \left[1 - \sum_n P_2^{\perp}(n)(1 - S_2^{\top\prime})^n\right]. \tag{5b}$$

The term in the first pair of square brackets on the right-hand side of Eq. (5b) denotes the probability that a hyperedge reached by a node-hyperedge connection in $\mathcal{G}_1$ belongs to the GCC of $\mathcal{G}_1$, and the term in the second pair of square brackets denotes the probability that the dependent hyperedge in the $\mathcal{G}_2$ belongs to the GCC of $\mathcal{G}_2$. Similarly, we have

$$S_2^{\top\prime} = \left[1 - \sum_l \frac{P_2^{\top}(l)l}{\langle l\rangle}(1 - S_2^{\perp\prime})^{l-1}\right], \tag{6a}$$

$$S_2^{\perp\prime} = \left[1 - \sum_n \frac{P_2^{\perp}(n)n}{\langle n\rangle}(1 - S_2^{\top\prime})^{n-1}\right] \times p^{\perp}\left[1 - \sum_m P_1^{\perp}(m)(1 - S_1^{\top\prime})^m\right]. \tag{6b}$$

Let $S_1^{\top}$ ($S_1^{\perp}$) and $S_2^{\top}$ ($S_2^{\perp}$) be the fraction of nodes (hyperedges) of $\mathcal{G}_1$ and $\mathcal{G}_2$ that are contained in the HMCGC, respectively, which serve as the proper order parameters to measure the robustness of the IH. With Eqs. (5) and (6), these order parameters can be calculated as follows:

$$\begin{aligned}
S_1^{\top} &= p^{\top}\left[1 - \sum_k P_1^{\top}(k)(1 - S_1^{\perp\prime})^k\right],\\
S_1^{\perp} &= p^{\perp}\left[1 - \sum_m P_1^{\perp}(m)(1 - S_1^{\top\prime})^m\right]\\
&\quad \times p^{\perp}\left[1 - \sum_n P_2^{\perp}(n)(1 - S_2^{\top\prime})^n\right],\\
S_2^{\top} &= 1 - \sum_k P_2^{\top}(l)(1 - S_2^{\perp\prime})^l,\\
S_2^{\perp} &= \left[1 - \sum_n P_2^{\perp}(n)(1 - S_2^{\top\prime})^n\right]\\
&\quad \times p^{\perp}\left[1 - \sum_m P_1^{\perp}(m)(1 - S_1^{\top\prime})^m\right].
\end{aligned} \tag{7}$$

In particular, when considering hypergraphs with Poisson degree distributions, Eq. (7) simplifies as

$$\begin{aligned}
S_1^{\top} &= p^{\top}(1 - e^{-\langle k\rangle S_1^{\perp\prime}}),\\
S_1^{\perp} &= p^{\perp}(1 - e^{-\langle m\rangle S_1^{\top\prime}})(1 - e^{-\langle n\rangle S_2^{\top\prime}}),\\
S_2^{\top} &= 1 - e^{-\langle l\rangle S_2^{\perp\prime}},\\
S_2^{\perp} &= (1 - e^{-\langle n\rangle S_2^{\top\prime}})p^{\perp}(1 - e^{-\langle m\rangle S_1^{\top\prime}}),
\end{aligned} \tag{8}$$

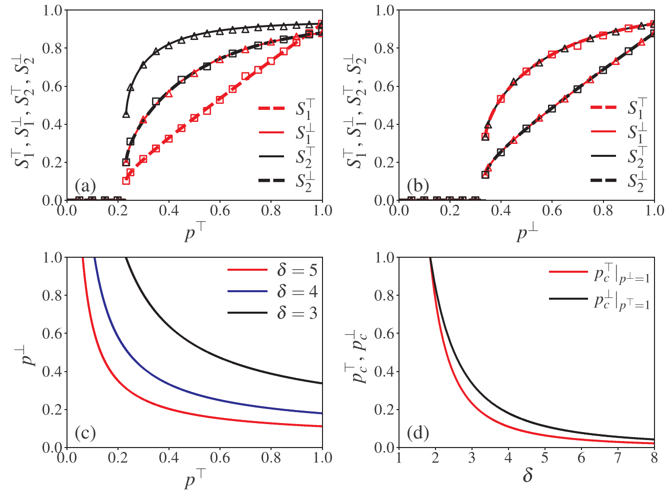

FIG. 3. Robustness of hyperedge-interdependent hypergraph. Order parameters $S_1^{\top}$, $S_1^{\perp}$, $S_2^{\top}$, and $S_2^{\perp}$ as functions of (a) $p^{\top}$ on the condition $p^{\perp} = 1$ and (b) $p^{\perp}$ on the condition $p^{\top} = 1$, where degree distributions satisfy Poisson distribution and all their average degrees equal $\delta = 3$. Symbols in (a) and (b) are obtained from numerical simulations. (c) The behaviors of the critical points $p_c^{\top}$ and $p_c^{\perp}$ on the $(p^{\top}, p^{\perp})$ plane for the cases $\langle k\rangle = \langle m\rangle = \langle l\rangle = \langle n\rangle = \delta = 3, 4, 5$, respectively. (d) Behaviors of $p_c^{\top}$ on the condition $p^{\perp} = 1$ and $p_c^{\perp}$ on the condition $p^{\top} = 1$ for growing values of the average degree δ.

with

$$\begin{aligned}
S_1^{\top\prime} &= p^{\top}(1 - e^{-\langle k\rangle S_1^{\perp\prime}}),\\
S_1^{\perp\prime} &= p^{\perp}(1 - e^{-\langle m\rangle S_1^{\top\prime}})(1 - e^{-\langle n\rangle S_2^{\top\prime}}),\\
S_2^{\top\prime} &= 1 - e^{-\langle l\rangle S_2^{\perp\prime}},\\
S_2^{\perp\prime} &= (1 - e^{-\langle n\rangle S_2^{\top\prime}})p^{\perp}(1 - e^{-\langle m\rangle S_1^{\top\prime}}),
\end{aligned} \tag{9}$$

where $\langle k\rangle$, $\langle m\rangle$, $\langle l\rangle$, and $\langle n\rangle$ are the average degree of the distributions $P_1^{\top}(k)$, $P_1^{\perp}(m)$, $P_2^{\top}(l)$, and $P_2^{\perp}(n)$, respectively.

Figure 3(a) shows the behaviors of the four order parameters along $p^{\top}$ on the condition $p^{\perp} = 1$ where $\langle k\rangle = \langle m\rangle = \langle l\rangle = \langle n\rangle = \delta$. In this case, the initial damage is imposed on the nodes of hypergraph $\mathcal{G}_1$. This leads to the severest damage on nodes of $\mathcal{G}_1$ as compared to other elements in $\mathcal{G}_1$ and $\mathcal{G}_2$, reflected by the lower curve that $S_1^{\top}$ has with respect to the other order parameters. Besides, we observe that the curves of $S_1^{\perp}$ (red solid) and $S_2^{\perp}$ (black dashed) completely overlap. This happens because the one-to-one correspondence of the hyperedge-dependency coupling mirrors the damage between the layers, resulting (on average) in the same number of remaining hyperedges in both hypergraphs. Moreover, since nodes in $\mathcal{G}_2$ receive minimal impact from the initial damage on the nodes in $\mathcal{G}_1$, the behavior of $S_2^{\top}$ is the largest among all the other order parameters. On the other hand, when initial damage acts on the hyperedges of $\mathcal{G}_1$ rather than the nodes, dependency links immediately mirror the damage to the hyperedges in $\mathcal{G}_2$ and, since these two hypergraphs have the same degree distribution, the fraction of percolating nodes is also the same for the two hypergraphs. Under these circumstances, we have that $S_1^{\perp} = S_2^{\perp}$ (damage on the hyperedges is the same) and $S_1^{\top} = S_2^{\top}$, as is shown in Fig. 3(b).

Percolation in IHs exhibits discontinuous phase transitions, as shown in Figs. 3(a) and 3(b). The procedure of evaluating the positions of the transition thresholds $p^\top = p_c^\top$ and $p^\perp = p_c^\perp$ is detailed in Appendix B. Since the initial damage acts only on $\mathcal{G}_1$, the reciprocal role of $p^\top$ and $p^\perp$ is no longer present, as visible from Eq. (10) below:

$$-bp^\perp(-acfp^\top p^\perp + adep^\top p^\perp + f) - acp^\top p^\perp + 1 = 0, \tag{10}$$

where the expressions of a–f can be found in Eq. (B2) in Appendix B. Figure 3(c) shows the relations of $p_c^\top$ and $p_c^\perp$ on the $(p^\top, p^\perp)$ plane for the cases of $\delta = 3, 4, 5$. We see that the robustness of IHs is enhanced by larger values of the average degree δ; moreover, the relative skewness of the curves, $p_c^\top|_{p^\perp=1} < p_c^\perp|_{p^\top=1}$, indicates that the system is, indeed, more tolerable to nodes' failure, given their lack of dependencies. This is further clarified by a more detailed plot of $p_c^\top|_{p^\perp=1}$ and $p_c^\perp|_{p^\top=1}$ in Fig. 3(d), where the former is always smaller than the latter.

IV. IH WITH INTERHYPERGRAPH CORRELATIONS

We consider now the case in which the degrees of two interdependent hyperedges are correlated. Specifically, we introduce a correlation function $P(m, n)$ which portrays the fraction of the interdependent hyperedges where one is of degree m in $\mathcal{G}_1$ and the other is of degree n in $\mathcal{G}_2$. Thus, we have $\sum_n P(m, n) = P_1^\perp(m)$ and $\sum_m P(m, n) = P_2^\perp(n)$.

Following a reasoning perfectly analogous to the one considered for Eqs. (5)–(7), we find

$$\begin{aligned}
S_1^{\top'} &= p^\top\left[1 - \sum_k \frac{P_1^\top(k)k}{\langle k\rangle}(1 - S_1^{\perp'})^{k-1}\right],\\
S_1^{\perp'} &= p^\perp \sum_{m,n} P(m, n)\left[1 - \frac{m}{\langle m\rangle}(1 - S_1^{\top'})^{m-1}\right]\\
&\quad \times [1 - (1 - S_2^{\top'})^n],\\
S_2^{\top'} &= \left[1 - \sum_l \frac{P_2^\top(l)l}{\langle l\rangle}(1 - S_2^{\perp'})^{l-1}\right],\\
S_2^{\perp'} &= p^\perp \sum_{m,n} P(m, n)\left[1 - \frac{n}{\langle n\rangle}(1 - S_2^{\top'})^{n-1}\right]\\
&\quad \times [1 - (1 - S_1^{\top'})^m],
\end{aligned} \tag{11}$$

and

$$\begin{aligned}
S_1^\top &= p^\top\left[1 - \sum_k P_1^\top(k)(1 - S_1^{\perp'})^k\right],\\
S_1^\perp &= p^\perp \sum_{m,n} P(m, n)[1 - (1 - S_1^{\top'})^m][1 - (1 - S_2^{\top'})^n],\\
S_2^\top &= \left[1 - \sum_l P_2^\top(l)(1 - S_2^{\perp'})^l\right],\\
S_2^\perp &= p^\perp \sum_{m,n} P(m, n)[1 - (1 - S_2^{\top'})^n][1 - (1 - S_1^{\top'})^m].
\end{aligned} \tag{12}$$

To quantify the impact of correlations on the robustness of IHs, we propose a method to generate the correlation function

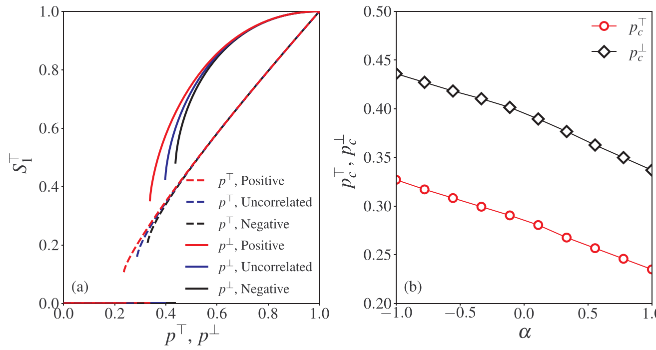

FIG. 4. Robustness of interdependent hypergraphs with hyperedge correlations. (a) Behaviors of $S_1^\top$ as functions of $p^\top$ with $p^\perp = 1$ (dashed curves) and $p^\perp$ with $p^\top = 1$ (solid curves) for a maximum positive correlation ($\alpha = 1$, red curves), noncorrelation ($\alpha = 0$, blue curves), and maximum negative correlation ($\alpha = -1$, black curves). (b) The relation between the critical points $p_c^\top$ or $p_c^\perp$ and the parameter α controlling the extent of hyperedge correlations. All the degree distributions of both hypergraphs follow identical power-law distribution, with the exponent being 2.2 and $\delta = 3$.

$P(m, n)$ which allows us to interpolate from the maximum degree of negative correlation to the maximum degree of positive correlation. For doing so, we first generate the maximum positive correlation function, denoted as $P^+(m, n)$. We list the hyperedges of the two hypergraphs both in ascending order according to their degree. Then, we establish dependency couplings for each pair of hyperedges that are collected from the two lists with the same index. Since both hypergraphs have the same number of hyperedges, a one-to-one correspondence is maintained. Evidently, such formed interdependency reaches the maximum extent of positive correlation. In a similar way, we can generate the maximum negative correlation function $P^-(m, n)$ by ordering the hyperedges of the two hypergraphs, one in ascending order and the other in descending order. Besides, a noncorrelation function $P^0(m, n)$ can be also defined via $P^0(m, n) = P_1^\perp(m)P_2^\perp(n)$. With these three functions, we define a correlation function $P(m, n)$ by introducing a controlling parameter $\alpha \in [-1, 1]$ which linearly tunes the weight of these functions as follows:

$$P(m, n) = \begin{cases} \alpha P^+(m, n) + (1 - \alpha)P^0(m, n), & \alpha \geqslant 0,\\ |\alpha|P^-(m, n) + (1 - |\alpha|)P^0(m, n), & \alpha < 0. \end{cases} \tag{13}$$

Notice that when $\alpha = 1, 0, -1$, $P(m, n)$ becomes $P^+(m, n)$, $P^0(m, n)$, and $P^-(m, n)$, respectively.

The effects of these correlations are presented in Fig. 4(a). We can see that for the cases of initial damage on nodes ($p^\top \leqslant 1$, $p^\perp = 1$, dashed curves) or initial damage on hyperedges ($p^\perp \leqslant 1$, $p^\top = 1$, solid curves), positive correlation produces the strongest robustness in both cases. On the one hand, positive correlations yield the smallest critical values $p_c^\top$ or $p_c^\perp$ so that, under such a pattern, the system may sustain the greatest extent of initial damage. On the other hand, positive correlations always result in the largest HMCGC (indicated by nonzero $S_1^\top$). These observations are further confirmed with the relation between the critical points $p_c^\top$ or $p_c^\perp$ and the controlling parameter α in Fig. 4(b). We find, in fact, that a larger α (greater extent of positive correlation) produces a smaller value of $p_c^\top$ and $p_c^\perp$. Moreover, we observe $p_c^\perp > p_c^\top$. This is because the initial damage on hyperedges will be immediately transferred to the dependent hyperedges in $\mathcal{G}_2$, which effectively doubles the initial damage, consistent with the results in Fig. 3(d).

V. NETWORK OF IHs WITH AN ARBITRARY NUMBER OF LAYERS

The bipartite network representation of IH can be conveniently extended to the case with an arbitrary number of interacting layers. We consider here an IH composed of L layers with all-to-all dependencies (denoted as L-IH). Every hypergraph has the same number of hyperedges and it is interdependent with every other $L-1$ hypergraph under one-to-one correspondence. When implementing dependency couplings, in particular, a feedback-loop condition is intended so that if hyperedge i in hypergraph 1 depends on hyperedge j in hypergraph 2 and hyperedge j in hypergraph 2 depends on hypergraph k in hypergraph 3, then hyperedge i must depend on hyperedge k. This avoids the additional amplification of a cascade through the spreading of damage caused by directed dependency patterns between the L hypergraphs.

Similarly to the case with $L=2$ IHs, a fully interdependent L-IH imposes here the condition $|\mathcal{N}_1^\perp| = \cdots = |\mathcal{N}_L^\perp|$ on the number of hyperedges in each layer. Hence, we denote the degree distributions of the ith hypergraph as $P_i^\top(k_i)$ and $P_i^\perp(m_i)$, respectively, and write the order parameters of the ith hypergraph as

$$
\begin{aligned}
S_i^\top &= (p^\top)^{\delta_{1i}} \mathbf{G}_{0i}^\top(1 - S_i^{\perp\prime}),\\
S_i^\perp &= (p^\perp) \prod_{j=1}^{L} \mathbf{G}_{0j}^\perp(1 - S_j^{\perp\prime}),
\end{aligned} \tag{14}
$$

with

$$
\begin{aligned}
S_i^{\top\prime} &= (p^\top)^{\delta_{1i}} \mathbf{G}_{1i}^\top(1 - S_i^{\perp\prime}),\\
S_i^{\perp\prime} &= (p^\perp) \mathbf{G}_{1i}^\perp(1 - S_i^{\top\prime}) \prod_{j=1, j\neq i}^{L} \mathbf{G}_{0j}^\perp(1 - S_j^{\perp\prime}),
\end{aligned} \tag{15}
$$

where $\delta_{1i} = 1$ when $i = 1$ and $\delta_{1i} = 0$ otherwise, and the generating functions $\mathbf{G}_{0i}^\top$, $\mathbf{G}_{0i}^\perp$, $\mathbf{G}_{1i}^\top$, and $\mathbf{G}_{1i}^\perp$ are defined as

$$
\begin{aligned}
\mathbf{G}_{0i}^\top(x) &= 1 - \sum_{k_i \geqslant 0} P_i^\top(k_i) x^{k_i},\\
\mathbf{G}_{0i}^\perp(x) &= 1 - \sum_{m_i \geqslant 0} P_i^\perp(m_i) x^{m_i},\\
\mathbf{G}_{1i}^\top(x) &= 1 - \sum_{k_i \geqslant 1} \frac{k_i P_i^\top(k_i)}{\langle k_i \rangle} x^{k_i - 1},\\
\mathbf{G}_{1i}^\perp(x) &= 1 - \sum_{m_i \geqslant 1} \frac{m_i P_i^\perp(m_i)}{\langle m_i \rangle} x^{m_i - 1}.
\end{aligned} \tag{16}
$$

Intuitively, since all the L hypergraphs are interdependent, a larger number of layers makes the whole IH more vulnerable to random damages [60]. This is indeed the case as verified by the behaviors of order parameter $S_1^\top$ as the functions of $p^\top$ (with $p^\perp = 1$) and of $p^\perp$ (with $p^\top = 1$) shown in Figs. 5(a) and 5(b), respectively, where the performance of degree-regular (DR) L-IH (degree of nodes and hyperedges of all the hypergraphs are identical) and uncorrelated power-law (UPL) L-IH (degree distributions of nodes and hyperedges of all the hypergraphs follow identical power-law distribution with no interhypergraph correlation) are presented. We observe that for both types of IHs, curves for larger L correspond to larger $p_c^\top$ and $p_c^\perp$ and smaller $S_1^\top$.

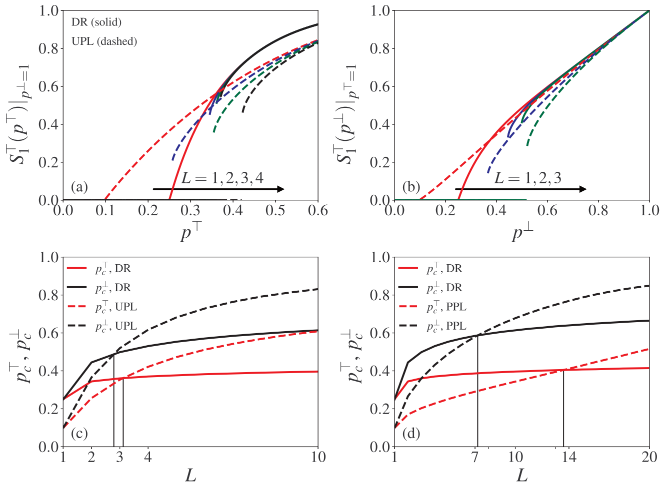

FIG. 5. Robustness of fully connected networks of hyperedge-interdependent hypergraphs. Behaviors of $S_1^\top$ as functions of (a) $p^\top$ (with $p^\perp = 1$) and (b) $p^\perp$ (with $p^\top = 1$) for different L on DR L-IH (solid curves), where all the nodes and hyperedges have the same degree, here being 3, and UPL L-IH (dashed curves), where all the degree distributions of nodes and hyperedges follow the same power-law distribution with the exponent being 2.8. The average degree of the power-law distribution is the same as that in DR L-IH. (c) Behaviors of critical points $p_c^\top$ and $p_c^\perp$ with the growing of L on DR L-IH and UPL L-IH. (d) Behaviors of critical points $p_c^\top$ and $p_c^\perp$ with the growing of L on the DR L-IH and power-law L-IH with maximum positive correlation (PPL L-IH).

Figures 5(a) and 5(b) convey, however, an interesting observation. When L is small, UPL L-IH possesses a smaller value of critical points $p_c^\top$ and $p_c^\perp$ than DR L-IH [red and blue curves in Fig. 5(a) and red curves in Fig. 5(b)], while when L is large, this situation reverses [green and black curves in Fig. 5(a) and blue and green curves in Fig. 5(b)]. This feature is more evident in Fig. 5(c), where the relation of critical points with the number L is presented. We can see that for both $p_c^\top$ (red) and $p_c^\perp$ (black) the curves for DR L-IH (solid) and UPL L-IH (dashed) intersect before or after $L = 3$. This feature could be understood in the way that heterogeneity of degree of nodes or hyperedges could enhance the robustness of the system, since hubs connect more elements in a hypergraph prone to form a large local clique. However, with the growing number of hypergraphs that are interdependent, a hub hyperedge becomes increasingly fragile due to the failure of its dependent hyperedges in other hypergraphs. Since hubs are rare, when a sufficient number of them fails, the UPL L-IH becomes rather fragile as the size of the remaining hyperedges is dominantly small. On the contrary, when instead the degree of hyperedges is homogeneous, the impact of losing a fraction of hyperedges is much less sensitive than the failure of hubs. Hence, the change in the value of critical points for DR L-IH is more stable (relatively small ranges of $p_c^\top$ and $p_c^\perp$) than that of UPL L-IH. This argument is further confirmed by comparing the behaviors of critical points between DR L-IH and power-law L-IH with maximum positive correlation (denoted as PPL L-IH) as shown in Fig. 5(d). A crossing between the curves for the two types of L-IH also appears, though the intersection point shifts to larger values of L due to stronger robustness induced by positive correlation.

VI. PARTIALLY INTERDEPENDENT HYPERGRAPHS

We here extend our bipartite framework to the case where only a fraction of hyperedges in a hypergraph are dependent on those in other hypergraphs; we refer to such cases as partially interdependent hypergraphs.

A. Partially interdependent hypergraphs with $L = 2$

We start by considering an IH composed of $L = 2$ layers. A fraction q_1 of hyperedges in hypergraph $\mathcal{G}_1$ is assumed to be interdependent with a fraction q_2 of hyperedges in $\mathcal{G}_2$ under the one-to-one fashion, in which case the self-consistent equations characterizing the system's order parameters are

$$
\begin{aligned}
S_1^{\top'} &= p^\top\left[1-\sum_k \frac{P_1^\top(k)k}{\langle k\rangle}(1-S_1^{\perp'})^{k-1}\right],\\
S_1^{\perp'} &= p^\perp\left\{q_1\left[1-\sum_m \frac{P_1^\perp(m)m}{\langle m\rangle}(1-S_1^{\top'})^{m-1}\right]\left[1-\sum_n P_2^\perp(n)(1-S_2^{\top'})^n\right]+(1-q_1)\left[1-\sum_m \frac{P_1^\perp(m)m}{\langle m\rangle}(1-S_1^{\top'})^{m-1}\right]\right\}\\
&= p^\perp\left[1-\sum_m \frac{P_1^\perp(m)m}{\langle m\rangle}(1-S_1^{\top'})^{m-1}\right]\left[1-q_1\sum_n P_2^\perp(n)\big(1-S_2^{\top'}\big)^n\right],\\
S_2^{\top'} &= \left[1-\sum_l \frac{P_2^\top(l)l}{\langle l\rangle}(1-S_2^{\perp'})^{l-1}\right],\\
S_2^{\perp'} &= p^\perp\left[1-\sum_n \frac{P_2^\perp(n)n}{\langle n\rangle}(1-S_2^{\top'})^{n-1}\right]\left[1-q_2\sum_m P_1^\perp(m)(1-S_1^{\top'})^m\right].
\end{aligned}
\tag{17}
$$

Since we aim at understanding the impact of partial dependency couplings, we adopt, for simplicity, Poisson distributions for the degree distributions of nodes and hyperedges with the same average degree δ, so that $\langle k\rangle = \langle m\rangle = \langle l\rangle = \langle n\rangle = \delta$. Because, in this case, the random removal of a fraction of nodes or hyperedges is equivalent to reducing the average degree of related distributions [31], we simplify the cascading process by setting $p^\top = p^\perp \equiv 1$, so that the impact of the initial damage is absorbed into the average degree δ. Given the identical average degree of the two hypergraphs, the one-to-one correspondence implies that $|\mathcal{N}_1^\perp| = |\mathcal{N}_2^\perp|$, meaning that $q_1 = q_2 \equiv q$. Then, Eq. (17) simplifies to

$$
\begin{aligned}
S_1^\top &= (1-e^{-\delta S_1^\perp}),\\
S_1^\perp &= (1-e^{-\delta S_1^\top})(1-qe^{-\delta S_2^\top}),\\
S_2^\top &= (1-e^{-\delta S_2^\perp}),\\
S_2^\perp &= (1-e^{-\delta S_2^\top})(1-qe^{-\delta S_1^\top}),
\end{aligned}
\tag{18}
$$

where the relations $S_1^\top = S_1^{\top'}$ and $S_2^\top = S_2^{\top'}$ have been adopted. Equation (18) indicates the symmetric relations between the order parameters for the two hypergraphs, which suggests the definition $S^\top = S_1^\top = S_2^\top$ and $S^\perp = S_1^\perp = S_2^\perp$. After some rearrangements, this yields the single self-consistent equation

$$
S^\top = 1 - e^{-\delta[(1-q)(1-e^{-\delta S^\top})+q(1-e^{-\delta S^\top})^2]}. \tag{19}
$$

Figure 6 presents the behavior of $S^\top(\delta)$ for several values of the fraction q of interdependent hyperedges. A continuous phase transition is observed in the weakly interdependent regime, i.e., when q is small (red dashed curve), followed by

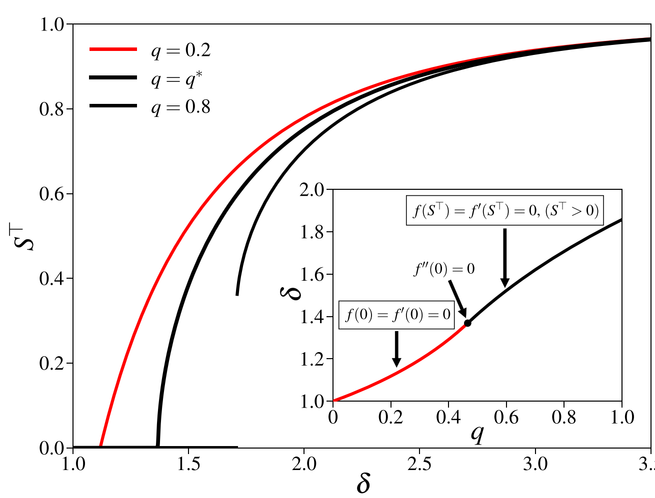

FIG. 6. Robustness of partially interdependent hypergraphs. Behaviors of the order parameter $S^\top$ as functions of δ for different q values ($q = q^*$ is the tricritical point). The inset shows the types of phase transitions on the (q, δ) plane: the red (black) curve corresponds to the continuous (discontinuous) phase transition, and the black dot identifies the tricritical point.

a discontinuous phase transition at larger values of q (black solid curve). Analogously to the case of partially interdependent pairwise networks [19–21,61], a tricritical point is also found in this case at a finite fraction $q = q^*$ and for an average degree $\delta = \delta^*$. To analytically determine the location of the tricritical point, we define the function $f(S^\top)$ with Eq. (19) as follows:

$$f(S^\top) = S^\top - (1 - e^{-\delta[(1-q)(1-e^{-\delta S^\top})+q(1-e^{-\delta S^\top})^2]}). \qquad (20)$$

A graphical analysis shows that continuous phase transitions occur when $f(0) = f'(0) = 0$, while discontinuous transitions happen whenever $f(S^\top) = f'(S^\top) = 0$ with $S^\top \geqslant 0$. The tricritical point is reached when the latter conditions coincide at $S^\top = 0$, i.e., $S^\top = f(S^\top) = f'(S^\top) = f''(S^\top) = 0$. The behaviors of the two types of phase transitions, as well as the location of the tricritical point on the (q, δ) plane, are shown in the inset of Fig. 6.

B. Partially interdependent hypergraphs with arbitrary L

We finally address the general case of a network of L partially interdependent hypergraphs. To simplify the analysis, we rely also here on the scenario where all the degree distributions of the hypergraphs Poisson with the same average degree $\delta \geqslant 1$. In this case, Eq. (18) can be generalized to

$$S_i^\top = 1 - e^{-\delta S_i^\perp},$$

$$S_i^\perp = (1-q)(1 - e^{-\delta S_i^\top}) + q\prod_{\ell=1}^{L}(1 - e^{-\delta S_\ell^\top}), \qquad (21)$$

where the definitions of the notations are inherited from Sec. VI A. Similarly, the symmetrical expressions of $S_i^\top$ and $S_i^\perp$ permit the definition $S^\top \equiv S_1^\top = \cdots = S_L^\top$ and $S^\perp \equiv S_1^\perp = \cdots = S_L^\perp$, which leads to

$$S^\top = 1 - \exp(-\delta[(1-q)(1 - e^{-\delta S^\top}) + q(1 - e^{-\delta S^\top})^L]), \qquad (22)$$

and hence the function $f(S^\top)$ reads now as

$$f(S^\top) = S^\top - (1 - e^{-\delta[(1-q)(1-e^{-\delta S^\top})+q(1-e^{-\delta S^\top})^L]}). \qquad (23)$$

Interestingly, the increase in the number of layers induces percolating behaviors that are absent in the $L = 2$ case. Figure 7(a) shows the behaviors of $S^\top(\delta)$ for several values of q for the case of $L = 3$. When q is relatively small, $S^\top(\delta)$ undergoes a continuous percolating phase transition. The condition for the onset of the continuous phase transition is $f(0) = f'(0) = 0$, which is indicated in the lower box in Fig. 7(b). However, when q surpasses the critical point $q_{\rm I}^*$, a region of *two-stage structural transitions* begins. The two-stage phase transition is a phenomenon in which both continuous and discontinuous phase transitions occur for the same q. Since the condition for the appearance of discontinuous phase transition is $f(S^\top) = f'(S^\top) = 0$, $(S^\top > 0)$, as indicated in the upper box in Fig. 7(b), this condition is also required for the appearance of the two-stage phase transition. However, more delicate conditions are further demanded for the existence of two-stage phase transition.

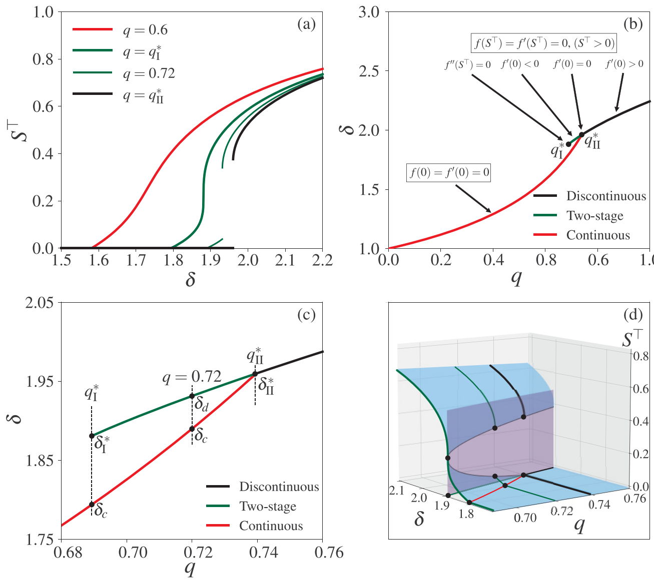

FIG. 7. Robustness of $L > 2$ partially interdependent hypergraphs. (a) Behaviors of the order parameter $S^\top$ for several values of q with $L = 3$; the red curve corresponds to the continuous transition, the green curve corresponds to the onset of the two-stage transition at $q = q_{\rm I}^* \simeq 0.69$ (with $\delta = \delta_{\rm I}^* \simeq 1.88$), the thin green curve exhibits a typical behavior of $S^\top$ with two-stage percolating transition, and the black curve corresponds to the onset of discontinuous transitions at $q_{\rm II}^* \simeq 0.74$ (with $\delta = \delta_{\rm II}^* \simeq 1.96$). (b) The three types of transitions are plotted on the (q, δ) plane, where red, green, and black curves match the definitions in (a). The conditions for the emergence of these structural transitions as well as the critical points $(q_{\rm I}^*, \delta_{\rm I}^*)$ and $(q_{\rm II}^*, \delta_{\rm II}^*)$ are presented and indicated by arrows. (c) Details of the parameters related to the two-stage phase transition, where $(q_{\rm I}^*, \delta_{\rm I}^*)$ and $(q_{\rm II}^*, \delta_{\rm II}^*)$ correspond to the onset and the end of the two-stage phase transition, respectively. (d) Three-dimensional plot of the behaviors $S^\top(q, \delta)$. The light blue surface indicates the profile of $S^\top$. The light purple curved plane intersects the profile at discontinuous phase transitions for reference. Black dots indicate typical locations of the phase transitions as in accordance with those in (c).

Specifically, at the critical point $q = q_{\rm I}^*$, when the growing δ first reaches the point δ_c satisfying the condition $f(0) = f'(0) = 0$, the *continuous* phase transition appears and the order parameter $S^\top$ starts to grow from zero to nonzero values in a continuous manner. Then, when δ further reaches the critical point $\delta_{\rm I}^*$ satisfying the condition $f(S^\top) = f'(S^\top) = 0$ [see Fig. 7(c)], a discontinuous phase transition with an infinitely small jump emerges [see Fig. 7(d)]. The coexistence of the two types of phase transitions at $q = q_{\rm I}^*$ indicates the emergence of the two-stage phase transition. A graphical analysis provided in Appendix C shows that this particular point demands an additional condition $f''(S^\top) = 0$. In other words, the condition for the onset of the two-stage phase transition is $f(S^\top) = f'(S^\top) = f''(S^\top) = 0$.

When $q = 0.72$, the two-stage phase transition is evident with $\delta = \delta_c$ corresponding to the *continuous* phase transitions and $\delta = \delta_d$ corresponding to the *discontinuous* phase transitions, as illustrated in Figs. 7(c) and 7(d). However, besides the conditions for the continuous and discontinuous phase transitions as expressed in the boxes in

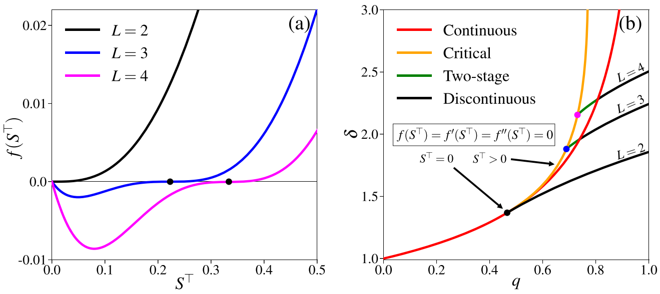

FIG. 8. Criterion for a two-stage structural transition in partially interdependent Poisson hypergraphs. (a) Behaviors of $f(S^\top)$ with $q = q_{\mathrm{I}}^*$ and $\delta = \delta_{\mathrm{I}}^*$ for the cases of $L = 2$, 3, and 4. Black dots indicate the nonzero solution of $S^\top$ that meets the condition $f(S^\top) = f'(S^\top) = f''(S^\top) = 0$ for $L = 3$ and 4. (b) Different types of phase transition are plotted on the $q - \delta$ plane. Specifically, the orange curve is obtained by solving $f(S^\top) = f'(S^\top) = f''(S^\top) = 0$ for different L values. This orange curve intersects with the curves for $L = 2$, 3, and 4 that are generated with the condition $f(S^\top) = f'(S^\top) = 0$. The three intersections (black, blue, and magenta dots) correspond to the curves in (a).

Fig. 7(b), the condition $f'(0) < 0$ is additionally required for the two-stage phase transition taking place at $q = 0.72$. When q further reaches the other critical point $q = q_{\mathrm{II}}^*$, the continuous phase transition terminates, signaled by the condition $f'(0) = 0$. As a consequence, the region of two-stage phase transition also terminates at this point, leaving only the classic discontinuous phase transition happening at $\delta = \delta_{\mathrm{II}}^*$. Relevant detailed graphical analysis can be found in Appendix C, which manifests that the emergence of a two-stage transition requires a nonzero solution $S^\top > 0$ for the condition $f(S^\top) = f'(S^\top) = f''(S^\top) = 0$. This is indeed satisfied if and only if $L > 2$ [see Fig. 8(a)] since, for $L = 2$, the solution for the condition is instead $S^\top = 0$, thus resulting in the absence of a two-stage transition.

The role of L in determining the existence of a nonzero solution $S^\top$ can be proved mathematically by analyzing the function $f(S^\top)$. Setting the condition $S^\top = f(S^\top) = f'(S^\top) = f''(S^\top) = 0$ in the definition (23), we get

$$1 + \delta = \delta^3 L(L-1) q (1 - e^{-\delta \cdot 0})^{L-2}, \tag{24}$$

where the relation $1 - \delta^2(1 - q) = 0$ obtained from $f'(0) = 0$ has been used. In fact, when $L > 2$, one finds $(1 - e^{-\delta \cdot 0})^{L-2} = 0$, so that Eq. (24) simplifies to $1 + \delta = 0$, which contradicts the requirement of $\delta > 0$ and therefore excludes $S^\top = 0$ from being a feasible solution for $L > 2$, implying a nonzero solution. However, when $L = 2$ the term $(1 - e^{-\delta \cdot 0})^{L-2}$ becomes an indeterminate form of the type 0^0, thus a reasonable solution of δ is possible when the indeterminate has a proper finite value. The orange curve in Fig. 8(b) shows the condition $f(S^\top) = f'(S^\top) = f''(S^\top) = 0$ and its dependence on L on the (q, δ) plane. We observe that this curve begins from $L = 2$, which intersects with the red curve (continuous phase transition); then, the two curves diverge, indicating the feasibility of two-stage phase transition when $L > 2$. We expect that similar arguments hold also for other cases where two-stage structural transitions have been reported—for example, in $L > 2$ multiplex networks with link overlap [25], as well as for percolation in duplex hypergraphs with large hyperedge cardinality [57].

VII. CONCLUSION

We have presented a bipartite network framework to study the robustness of IHs under various structural settings. In this representation, we have developed a theory based on the generating function formalism to describe the percolation process in IHs. We have demonstrated the generality of our framework by applying it to various cases, including correlated IHs, IHs with an arbitrary number of layers, and partially IHs. The impact on the robustness of IHs of hyperedges, of the extent of correlation between hyperedges in different hypergraphs, of the number of hypergraphs, and of the degree of partial interdependency has been studied in detail. One of the most important findings refers to the identification in the condition of producing a two-stage phase transition in partially IH, which can only happen when more than two hypergraphs are partially dependent in a system. Our findings deepen the understanding on this topic and advance the development of the theory of interdependent systems. We stress that, while our framework exhaustively takes into account the aftermath (i.e., the equilibrium phases) due to cascading failures in interdependent hypergraphs, it does not provide information about the temporal evolution of the percolating observables during the propagation of cascades, which we find to be a desirable direction for future works. We hope, hence, that our work brings useful insights also for the study of higher-order systems with the potential to be generalized to scenarios where hypergraphs have richer structural and dynamical features.

ACKNOWLEDGMENTS

This work was supported in part by the National Natural Science Foundation of China (Grants No. 11835003 and No. 12075088) and the Natural Science Foundation of Zhejiang Province (Grant No. Y22F035316). I.B. acknowledges funding from ERC Grant No. 810115-DYNASET.

APPENDIX A: BIPARTITE REPRESENTATION OF ISOLATED HYPERGRAPHS

1. Site-bond percolation on random networks

We first derive the equations for site-bond percolation on random pairwise networks based on the generating function formalism. We call, respectively, $p^\top$ and $p^\perp$ the occupation probability of nodes and of edges of a given network with degree distribution $P(k)$. We perform a random site-bond percolation by removing, independently from each other, a fraction $1 - p^\top$ of nodes and a fraction $1 - p^\perp$ of edges. Under the condition that the network is locally tree-like, we can solve exactly the site-bond percolation problem in a recursive fashion as follows. Let u be the probability that, following a randomly chosen edge to one of its vertices whose degree is k, we arrive at a finite connected component; since we percolate both bonds and sites, u is given by the mean over the network of the sum of three main contributions: (1) the probability that the edge itself is empty, $1 - p^\perp$; (2) the probability that the edge is occupied but the vertex we arrive is empty,

$p^\perp(1-p^\top)$; and (3) the probability that the bond is occupied and the vertex is occupied but none of the $k-1$ remaining edges leads to the giant connected component, $p^\top p^\perp u^{k-1}$. Summing the above and performing an average over the network, we find

$$u = 1 - p^\top p^\perp + p^\top p^\perp \sum_{k\geqslant 1} \frac{kP(k)}{\langle k\rangle} u^{k-1}, \tag{A1}$$

which can be equivalently rewritten in terms of the complementary probability $x \equiv 1-u$ as

$$x = p^\top p^\perp \left(1 - \sum_{k\geqslant 1} \frac{kP(k)}{\langle k\rangle}(1-x)^{k-1}\right). \tag{A2}$$

The probability, $1-S$, that a randomly chosen node does not belong to the giant connected component is, instead, the sum of two terms: (1) the probability that the site is empty, $1-p^\top$, and (2) the probability that the site is occupied but none of its k emanating edges leads to the giant, i.e., $p^\top u^k$. Again, adopting the tree-like approximation, we get

$$S = p^\top\left(1 - \sum_{k\geqslant 0} P(k)u^k\right). \tag{A3}$$

We now show how the above problem can be equivalently solved within the bipartite network representation. To this aim, we define $P(k)$ the degree distribution of "site" nodes and with $P(m)$ the degree distribution of the "edge" nodes. Since the network still retains its locally tree-like structure, let us define $u_\top$ (respectively, $u_\perp$) the probability that by following a randomly chosen edge of the bipartite representation we arrive at a site node (respectively, an edge node) that does not belong to the giant component of the network. Given the perfect equivalence between site nodes and edge nodes, the arguments in the above readily follow and imply that the probability that a randomly chosen site node $S^\top$ or edge node $S^\perp$ are respectively given by

$$\begin{aligned} S^\top &= p^\top\left(1 - \sum_{k\geqslant 0} P(k)u_\perp^k\right),\\ S^\perp &= p^\perp\left(1 - \sum_{m\geqslant 0} P(m)u_\top^m\right), \end{aligned} \tag{A4}$$

where the probabilities $u_\top$ and $u_\perp$ are, *mutatid mutandis*, given by

$$\begin{aligned} u_\top &= 1 - p^\top + p^\top \sum_{k\geqslant 1} \frac{kP(k)}{\langle k\rangle} u_\perp^{k-1},\\ u_\perp &= 1 - p^\perp + p^\perp \sum_{m\geqslant 1} \frac{mP(m)}{\langle m\rangle} u_\top^{m-1}. \end{aligned} \tag{A5}$$

To verify that Eqs. (A4) and (A5) match Eqs. (A1)–(A3), it is sufficient to notice that, for pairwise graphs, $P(m) = \delta_{m,2}$, with δ_{mn} the Kronecker delta distribution function, so $u_\perp = 1 - p^\perp + p^\perp u_\top = 1 - p^\perp(1-u_\top)$. By calling $y_\top \equiv 1 - u_\top$ and identifying $x_\top \equiv p^\perp y_\top$, one recovers Eq. (A2) from $u_\top$ in Eq. (A5) and Eq. (A3) from $S^\top$ in Eq. (A4).

2. Percolation critical threshold

The critical points $p_c^\top$ and $p_c^\perp$ for a single hypergraph could be calculated by the Jacobian matrix obtained from Eqs. (1) and (2) at the point $S_1^{\top'} = S_1^{\perp'} = 0$. The nonzero elements of the Jacobian matrix can be expressed as follows:

$$\begin{aligned} \left.\frac{\partial S_1^{\top'}}{\partial S_1^{\perp'}}\right|_{S_1^{\perp'}=0} &= p^\top \frac{\langle k(k-1)\rangle}{\langle k\rangle},\\ \left.\frac{\partial S_1^{\perp'}}{\partial S_1^{\top'}}\right|_{S_1^{\top'}=0} &= p^\perp \frac{\langle m(m-1)\rangle}{\langle m\rangle}. \end{aligned} \tag{A6}$$

Then, imposing the condition that the largest eigenvalue Λ of the matrix equals 1,

$$\det[\mathbf{J}-\mathbf{I}] = \begin{vmatrix} -\Lambda & p^\top \frac{\langle k(k-1)\rangle}{\langle k\rangle} \\ p^\perp \frac{\langle m(m-1)\rangle}{\langle m\rangle} & -\Lambda \end{vmatrix} = 0, \tag{A7}$$

where $\mathbf{I}$ is the unit matrix. Equation (A7) produces the relation of the critical points $p_c^\top$ and $p_c^\perp$, which reads

$$p_c^\top p_c^\perp = \left[\frac{\langle m(m-1)\rangle}{\langle m\rangle}\frac{\langle k(k-1)\rangle}{\langle k\rangle}\right]^{-1}. \tag{A8}$$

APPENDIX B: THEORETICAL EVALUATION OF CRITICAL POINTS FOR IH COMPOSED OF TWO HYPERGRAPHS

Equations (5) and (6) are shown in Eq. (B1) below for convenience, which allow to compute the critical points $p_c^\top$ and $p_c^\perp$ of an interdependent hypergraph.

$$\begin{aligned} S_1^{\top'} &= p^\top\left[1 - \sum_k \frac{P_1^\top(k)k}{\langle k\rangle}(1-S_1^{\perp'})^{k-1}\right],\\ S_2^{\top'} &= \left[1 - \sum_l \frac{P_2^\top(l)l}{\langle l\rangle}(1-S_2^{\perp'})^{l-1}\right],\\ S_1^{\perp'} &= p^\perp\left[1 - \sum_m \frac{P_1^\perp(m)m}{\langle m\rangle}(1-S_1^{\top'})^{m-1}\right]\left[1 - \sum_n P_2^\perp(n)(1-S_2^{\top'})^n\right],\\ S_2^{\perp'} &= \left[1 - \sum_n \frac{P_2^\perp(n)n}{\langle n\rangle}(1-S_2^{\top'})^{n-1}\right]p^\perp\left[1 - \sum_m P_1^\perp(m)(1-S_1^{\top'})^m\right]. \end{aligned} \tag{B1}$$

For doing so, we calculate the Jacobian matrix of Eq. (B1), and its nonzero elements are presented in Eq. (B2) with the notation $\partial_{\perp,j}^{\top,i} = \frac{\partial S_i^{\top'}}{\partial S_j^{\perp'}}$,

$$\begin{aligned}
\partial_{\perp,1}^{\top,1} &= p^{\top} \sum_k \frac{P_1^{\top}(k)k(k-1)}{\langle k\rangle}(1-S_1^{\perp'})^{k-2} &&= p^{\top} a,\\
\partial_{\perp,2}^{\top,2} &= \sum_l \frac{P_2^{\top}(l)l(l-1)}{\langle l\rangle}(1-S_2^{\perp'})^{l-2} &&= b,\\
\partial_{\top,1}^{\perp,1} &= p^{\perp} \sum_m \frac{P_1^{\perp}(m)m(m-1)}{\langle m\rangle}(1-S_1^{\top'})^{m-2}\left[1-\sum_n P_2^{\perp}(n)(1-S_2^{\top'})^n\right] &&= p^{\perp} c,\\
\partial_{\top,2}^{\perp,1} &= p^{\perp}\left[1-\sum_m \frac{P_1^{\perp}(m)m}{\langle m\rangle}(1-S_1^{\top'})^{m-1}\right]\sum_n P_2^{\perp}(n)n(1-S_2^{\top'})^{n-1} &&= p^{\perp} d,\\
\partial_{\top,1}^{\perp,2} &= p^{\perp}\left[1-\sum_n \frac{P_2^{\perp}(n)n}{\langle n\rangle}(1-S_2^{\top'})^{n-1}\right]\sum_m P_1^{\perp}(m)m(1-S_1^{\top'})^{m-1} &&= p^{\perp} e,\\
\partial_{\top,2}^{\perp,2} &= p^{\perp} \sum_n \frac{P_2^{\perp}(n)n(n-1)}{\langle n\rangle}(1-S_2^{\top'})^{n-2}\left[1-\sum_m P_1^{\perp}(m)(1-S_1^{\top'})^m\right] &&= p^{\perp} f.
\end{aligned} \tag{B2}$$

The critical points $p_c^{\top}$ and $p_c^{\perp}$ satisfy the condition when the largest eigenvalue of the Jacobian matrix equals 1, i.e., $\Lambda = 1$. The secular equation of the Jacobian matrix is written as

$$\begin{aligned}
\det[\mathbf{J}-\mathbf{I}] &= \begin{vmatrix} -\Lambda & 0 & \partial_{\perp,1}^{\top,1} & 0 \\ 0 & -\Lambda & 0 & \partial_{\perp,2}^{\top,2} \\ \partial_{\top,1}^{\perp,1} & \partial_{\top,2}^{\perp,1} & -\Lambda & 0 \\ \partial_{\top,1}^{\perp,2} & \partial_{\top,2}^{\perp,2} & 0 & -\Lambda \end{vmatrix} \\
&= \Lambda^4 - \left(\partial_{\perp,1}^{\top,1}\partial_{\top,1}^{\perp,1} + \partial_{\perp,2}^{\top,2}\partial_{\top,2}^{\perp,2}\right)\Lambda^2 + \partial_{\perp,1}^{\top,1}\partial_{\perp,2}^{\top,2}\left(\partial_{\top,1}^{\perp,1}\partial_{\top,2}^{\perp,2} - \partial_{\top,2}^{\perp,1}\partial_{\top,1}^{\perp,2}\right) = 0.
\end{aligned} \tag{B3}$$

Letting $\Lambda = 1$, one gets

$$\begin{aligned}
&\partial_{\perp,1}^{\top,1}\partial_{\perp,2}^{\top,2}\left(\partial_{\top,2}^{\perp,1}\partial_{\top,1}^{\perp,2} - \partial_{\top,1}^{\perp,1}\partial_{\top,2}^{\perp,2}\right) + \partial_{\perp,1}^{\top,1}\partial_{\top,1}^{\perp,1} + \partial_{\perp,2}^{\top,2}\partial_{\top,2}^{\perp,2} - 1 \\
&\quad = 0,
\end{aligned} \tag{B4}$$

which gives

$$-bp^{\perp}(-acf p^{\top}p^{\perp} + adep^{\top}p^{\perp} + f) - acp^{\top}p^{\perp} + 1 = 0. \tag{B5}$$

Equation (B5) shows that $p^{\top}$ and $p^{\perp}$ do not always appear in pairs, indicating their asymmetric roles in interdependent hypergraphs.

APPENDIX C: GRAPHICAL ANALYSIS OF TYPICAL PERCOLATING BEHAVIORS STUDIED IN SEC. VI B

To provide more detailed understanding about why two-stage transition is absent for $L = 2$ but emerge when more layers are coupled together, we investigate the four different percolation behaviors of $S^{\top}(\delta)$ for $L = 3$ presented in Fig. 7(a) by analyzing corresponding behaviors of the function $f(S^{\top})$.

Figure 9(b) shows the behaviors of $f(S^{\top})$ for three typical δ values as indicated by the vertical lines in Fig. 9(a), where the red curve in Fig. 9(a) is duplicated from that in Fig. 7(a). The shape of $f(S^{\top})$ illustrates that with the growing of δ, the (stable) solution of $f(S^{\top}) = 0$ continuously grows from zero to nonzero values. The condition for the appearance of continuous phase transition is $f(0) = f'(0) = 0$, which is consistent with the results in Ref. [61].

The behaviors of $f(S^{\top})$ for the case of $q = q_{\mathrm{I}}^*$ for typical δ values are presented in Fig. 9(d). It is obvious that in this case the shape of $f(S^{\top})$ is essentially different from those in Fig. 9(b). One may observe that these curves possess a special point in the medium range of $S^{\top}$ at which $f''(S^{\top}) = 0$ (denoted by black dots). In particular, for the special case $\delta = \delta_{\mathrm{I}}^*$ the nonzero solution of $f(S^{\top}) = 0$ locates exactly at the point when $f''(S^{\top}) = 0$ as well as $f'(S^{\top}) = 0$ (the orange curve).

In fact, the nonzero solution of the condition $f(S^{\top}) = f'(S^{\top}) = f''(S^{\top}) = 0$ signals the emergence of a two-stage phase transition. This can be better understood by observing Figs. 9(e) and 9(f) for the case of $q = 0.72$, where a typical two-stage phase transition is evidently exhibited. We can see that at the critical point $\delta = \delta_d$ where a discontinuous phase transition takes place, there are two nonzero solutions for the $f(S^{\top})$, one for continuous phase transition (the smaller one) and one for discontinuous phase transition (the larger one). Note that the larger one [the right dot in Fig. 9(f)] meets the condition $f(S^{\top}) = f'(S^{\top}) = 0$, which is the requisite for the appearance of discontinuous phase transition. Further, by comparing Figs. 9(d) and 9(f), one may expect that with the decreasing of q, the two black dots in Fig. 9(f) will approach

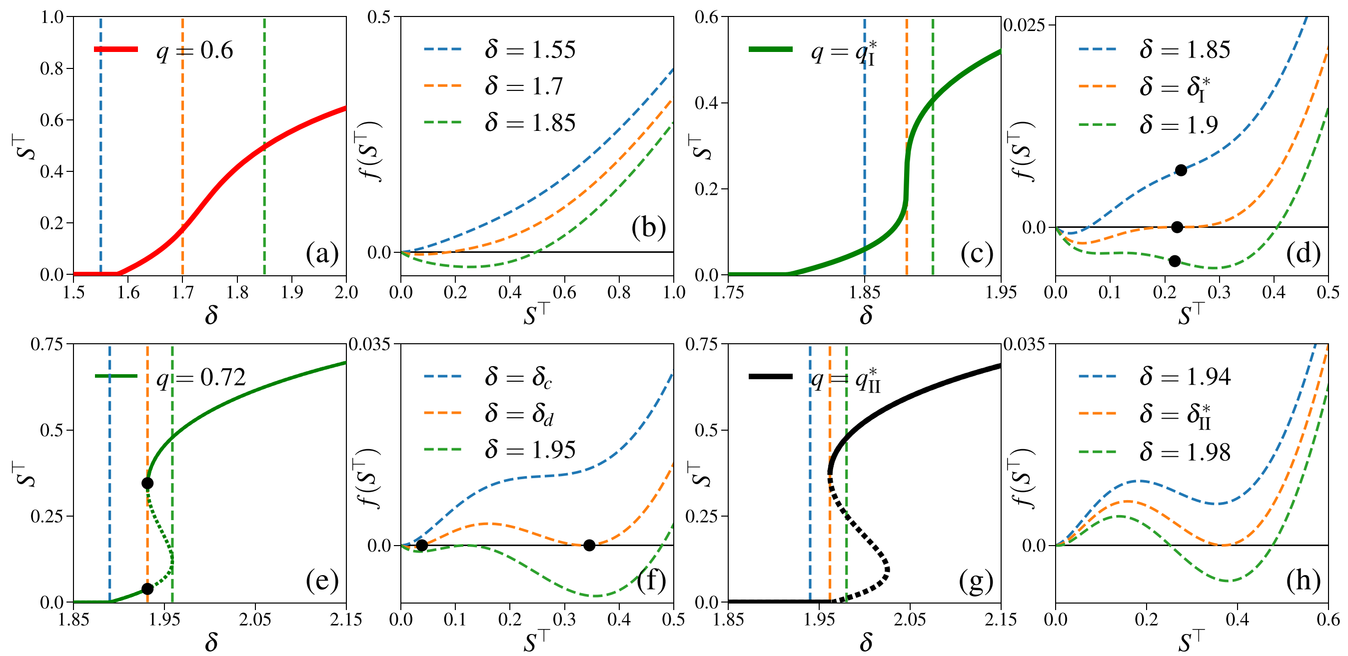

FIG. 9. Graphical analysis of the function $f(S^\top)$ for typical percolation behaviors for $L = 3$ as shown in Fig. 7(a). (a) The behavior of $S^\top(\delta)$ for the case of $q = 0.6$ [the same as the red curve in Fig. 7(a)], where blue, orange, and green dashed vertical lines indicate three typical δ values. (b) Behaviors of the function $f(S^\top)$ for the three typical δ values identified in (a). Similarly, (c) and (d), (e) and (f), and (g) and (h) present the behaviors of $S^\top(\delta)$ and $f(S^\top)$ of typical δ values for the cases of $q = q_{\mathrm{I}}^*$, $q = 0.72$, and $q = q_{\mathrm{II}}^*$, respectively. The black dots in (d) indicate the location of $f''(S^\top) = 0$. The black dots in (e) and (f) indicate the two nonzero solutions of $f(S^\top) = 0$. $\delta_c \simeq 1.89$ ($\delta_d \simeq 1.93$) in (f) indicates the critical value of δ where the continuous (discontinues) phase transition happens.

and finally merge together, resulting in the orange curve in Fig. 9(d). At this particular situation $f''(S^\top) = 0$ is attained, and the two types of phase transition are merged to a continuous phase transition. Thus, the condition $f(S^\top) = f'(S^\top) = f''(S^\top) = 0$ determines the the lower boundary of q, i.e., $q = q_{\mathrm{I}}^*$, for the appearance of the two-stage phase transition. On the other hand, with the increasing of q, the two black dots will move apart, and at the point $q = q_{\mathrm{II}}^*$ the left dot will reach the original point [giving $f'(0) = 0$] where the two-stage phase transition simplifies to the classic discontinuous phase transition, which indicates the upper boundary of q for the two-stage phase transition [see Figs. 9(g) and 9(h)].

Hence, the above observations suggest the following understanding: (i) When q is in a medium range of $q_{\mathrm{I}}^* \leqslant q \leqslant q_{\mathrm{II}}^*$ [for example, $q = 0.72$ in Fig. 9(e)], on the condition δ is in the range $\delta_c < \delta < \delta_d$, the fraction $1 - q$ of the independent part in each hypergraph appended with some small fraction of dependent hyperedges is enough to formed a nonzero (but relatively small) size of HMCGC, which supports that a continuous phase transition occurred at δ_c. When δ reaches δ_d, a discontinuous phase transition occurs due to the interdependency. These combined effects contribute to a two-stage phase transition. (ii) When q is small ($q < q_{\mathrm{I}}^*$), the fraction $1 - q$ of independent part is large enough that the HMCGC is formed mainly on the basis of the independent part of hypergraphs and the effect of the interdependency is submerged into the existing HMCGC with the growing of δ. In this case, the discontinuous phase transition is invisible, leaving only a continuous phase transition to the system. (iii) When q is large ($q > q_{\mathrm{II}}^*$), on the condition a discontinuous phase transition happens at $\delta = \delta_d$, the fraction of the independent part is, however, so small that a HMCGC is not formed yet, resulting in a single discontinuous phase transition.

[1] M. De Domenico, A. Solé-Ribalta, E. Cozzo, M. Kivelä, Y. Moreno, M. A. Porter, S. Gómez, and A. Arenas, Mathematical formulation of multilayer networks, Phys. Rev. X **3**, 041022 (2013).

[2] S. Boccaletti, G. Bianconi, R. Criado, C. I. Del Genio, J. Gómez-Gardenes, M. Romance, I. Sendina-Nadal, Z. Wang, and M. Zanin, The structure and dynamics of multilayer networks, Phys. Rep. **544**, 1 (2014).

[3] G. Bianconi, *Multilayer Networks: Structure and Function* (Oxford University Press, New York, 2018).

[4] M. De Domenico, More is different in real-world multilayer networks, Nat. Phys. **19**, 1247 (2023).

[5] J. C. Rocha, G. Peterson, Ö. Bodin, and S. Levin, Cascading regime shifts within and across scales, Science **362**, 1379 (2018).

[6] R. V. Solé, M. Rosas-Casals, B. Corominas-Murtra, and S. Valverde, Robustness of the European power grids under intentional attack, Phys. Rev. E **77**, 026102 (2008).

[7] Y. Yang, T. Nishikawa, and A. E. Motter, Small vulnerable sets determine large network cascades in power grids, Science **358**, eaan3184 (2017).

[8] B. Schäfer, D. Witthaut, M. Timme, and V. Latora, Dynamically induced cascading failures in power grids, Nat. Commun. **9**, 1975 (2018).

[9] T. Nesti, F. Sloothaak, and B. Zwart, Emergence of scale-free blackout sizes in power grids, Phys. Rev. Lett. **125**, 058301 (2020).

[10] A. M. Amani and M. Jalili, Power grids as complex networks: Resilience and reliability analysis, IEEE Access **9**, 119010 (2021).

[11] R. M. May, S. A. Levin, and G. Sugihara, Ecology for bankers, Nature (London) **451**, 893 (2008).

[12] A. G. Haldane and R. M. May, Systemic risk in banking ecosystems, Nature (London) **469**, 351 (2011).

[13] M. Scheffer, *Critical Transitions in Nature and Society* (Princeton University Press, Princeton, 2020), Vol. 16.

[14] M. Diao, H. Kong, and J. Zhao, Impacts of transportation network companies on urban mobility, Nat. Sustainability **4**, 494 (2021).

[15] W. Lei, L. G. Alves, and L. A. N. Amaral, Forecasting the evolution of fast-changing transportation networks using machine learning, Nat. Commun. **13**, 4252 (2022).

[16] N. P. Simpson, K. J. Mach, A. Constable, J. Hess, R. Hogarth, M. Howden, J. Lawrence, R. J. Lempert, V. Muccione, B. Mackey *et al.*, A framework for complex climate change risk assessment, One Earth **4**, 489 (2021).

[17] L. Kemp, C. Xu, J. Depledge, K. L. Ebi, G. Gibbins, T. A. Kohler, J. Rockström, M. Scheffer, H. J. Schellnhuber, W. Steffen *et al.*, Climate endgame: Exploring catastrophic climate change scenarios, Proc. Natl. Acad. Sci. USA **119**, e2108146119 (2022).

[18] S. V. Buldyrev, R. Parshani, G. Paul, H. E. Stanley, and S. Havlin, Catastrophic cascade of failures in interdependent networks, Nature (London) **464**, 1025 (2010).

[19] R. Parshani, S. V. Buldyrev, and S. Havlin, Interdependent networks: Reducing the coupling strength leads to a change from a first to second order percolation transition, Phys. Rev. Lett. **105**, 048701 (2010).

[20] J. Gao, S. V. Buldyrev, H. E. Stanley, and S. Havlin, Networks formed from interdependent networks, Nat. Phys. **8**, 40 (2012).

[21] A. Bashan, Y. Berezin, S. V. Buldyrev, and S. Havlin, The extreme vulnerability of interdependent spatially embedded networks, Nat. Phys. **9**, 667 (2013).

[22] I. Bonamassa, B. Gross, M. Laav, I. Volotsenko, A. Frydman, and S. Havlin, Interdependent superconducting networks, Nat. Phys. **19**, 1163 (2023).

[23] G. Dong, J. Gao, L. Tian, R. Du, and Y. He, Percolation of partially interdependent networks under targeted attack, Phys. Rev. E **85**, 016112 (2012).

[24] L. D. Valdez, P. A. Macri, H. E. Stanley, and L. A. Braunstein, Triple point in correlated interdependent networks, Phys. Rev. E **88**, 050803(R) (2013).

[25] D. Cellai, E. López, J. Zhou, J. P. Gleeson, and G. Bianconi, Percolation in multiplex networks with overlap, Phys. Rev. E **88**, 052811 (2013).

[26] L. M. Shekhtman, S. Shai, and S. Havlin, Resilience of networks formed of interdependent modular networks, New J. Phys. **17**, 123007 (2015).

[27] K.-K. Kleineberg, M. Boguná, M. Ángeles Serrano, and F. Papadopoulos, Hidden geometric correlations in real multiplex networks, Nat. Phys. **12**, 1076 (2016).

[28] F. Radicchi and G. Bianconi, Redundant interdependencies boost the robustness of multiplex networks, Phys. Rev. X **7**, 011013 (2017).

[29] J. Gao, S. V. Buldyrev, S. Havlin, and H. E. Stanley, Robustness of a network of networks, Phys. Rev. Lett. **107**, 195701 (2011).

[30] J. Shao, S. V. Buldyrev, S. Havlin, and H. E. Stanley, Cascade of failures in coupled network systems with multiple support-dependence relations, Phys. Rev. E **83**, 036116 (2011).

[31] H. Zhang, J. Zhou, Y. Zou, M. Tang, G. Xiao, and H. E. Stanley, Asymmetric interdependent networks with multiple-dependence relation, Phys. Rev. E **101**, 022314 (2020).

[32] R. Lambiotte, M. Rosvall, and I. Scholtes, From networks to optimal higher-order models of complex systems, Nat. Phys. **15**, 313 (2019).

[33] F. Battiston, G. Cencetti, I. Iacopini, V. Latora, M. Lucas, A. Patania, J.-G. Young, and G. Petri, Networks beyond pairwise interactions: structure and dynamics, Phys. Rep. **874**, 1 (2020).

[34] F. Battiston, E. Amico, A. Barrat, G. Bianconi, G. Ferraz de Arruda, B. Franceschiello, I. Iacopini, S. Kéfi, V. Latora, Y. Moreno *et al.*, The physics of higher-order interactions in complex systems, Nat. Phys. **17**, 1093 (2021).

[35] G. Bianconi, *Higher-Order Networks* (Cambridge University Press, New York, 2021).

[36] R. Ghorbanchian, V. Latora, and G. Bianconi, Hyper-diffusion on multiplex networks, J. Phys.: Complexity **3**, 035009 (2022).

[37] Y. Zhang, M. Lucas, and F. Battiston, Higher-order interactions shape collective dynamics differently in hypergraphs and simplicial complexes, Nat. Commun. **14**, 1605 (2023).

[38] L. Calmon, M. Schaub, and G. Bianconi, Dirac signal processing of higher-order topological signals, New J. Phys. **25**, 093013 (2023).

[39] J. Grilli, G. Barabás, M. J. Michalska-Smith, and S. Allesina, Higher-order interactions stabilize dynamics in competitive network models, Nature (London) **548**, 210 (2017).

[40] A. P. Millán, J. J. Torres, and G. Bianconi, Explosive higher-order Kuramoto dynamics on simplicial complexes, Phys. Rev. Lett. **124**, 218301 (2020).

[41] J. T. Matamalas, S. Gómez, and A. Arenas, Abrupt phase transition of epidemic spreading in simplicial complexes, Phys. Rev. Res. **2**, 012049(R) (2020).

[42] H. Guo, D. Jia, I. Sendiña-Nadal, M. Zhang, Z. Wang, X. Li, K. Alfaro-Bittner, Y. Moreno, and S. Boccaletti, Evolutionary games on simplicial complexes, Chaos Solit. Fractals **150**, 111103 (2021).

[43] L. V. Gambuzza, F. Di Patti, L. Gallo, S. Lepri, M. Romance, R. Criado, M. Frasca, V. Latora, and S. Boccaletti, Stability of synchronization in simplicial complexes, Nat. Commun. **12**, 1255 (2021).

[44] R. Ghorbanchian, J. G. Restrepo, J. J. Torres, and G. Bianconi, Higher-order simplicial synchronization of coupled topological signals, Commun. Phys. **4**, 120 (2021).

[45] S. Majhi, M. Perc, and D. Ghosh, Dynamics on higher-order networks: A review, J. R. Soc. Interface. **19**, 20220043 (2022).

[46] T. Carletti, L. Giambagli, and G. Bianconi, Global topological synchronization on simplicial and cell complexes, Phys. Rev. Lett. **130**, 187401 (2023).

[47] I. Iacopini, G. Petri, A. Barrat, and V. Latora, Simplicial models of social contagion, Nat. Commun. **10**, 2485 (2019).

[48] Z. Li, Z. Deng, Z. Han, K. Alfaro-Bittner, B. Barzel, and S. Boccaletti, Contagion in simplicial complexes, Chaos Solit. Fractals **152**, 111307 (2021).

[49] A. Barrat, G. Ferraz de Arruda, I. Iacopini, and Y. Moreno, Social contagion on higher-order structures, in *Higher-Order Systems* (Springer, New York, 2022), pp. 329–346.

[50] E. Bairey, E. D. Kelsic, and R. Kishony, High-order species interactions shape ecosystem diversity, Nat. Commun. **7**, 12285 (2016).

[51] J. M. Levine, J. Bascompte, P. B. Adler, and S. Allesina, Beyond pairwise mechanisms of species coexistence in complex communities, Nature (London) **546**, 56 (2017).

[52] P. Singh and G. Baruah, Higher order interactions and species coexistence, Theor. Ecol. **14**, 71 (2021).

[53] T. Gibbs, S. A. Levin, and J. M. Levine, Coexistence in diverse communities with higher-order interactions, Proc. Natl. Acad. Sci. USA **119**, e2205063119 (2022).

[54] D. Zhao, R. Li, H. Peng, M. Zhong, and W. Wang, Higher-order percolation in simplicial complexes, Chaos Solit. Fractals **155**, 111701 (2022).

[55] F. Baccini, F. Geraci, and G. Bianconi, Weighted simplicial complexes and their representation power of higher-order network data and topology, Phys. Rev. E **106**, 034319 (2022).

[56] H. Peng, Z. Xie, D. Zhao, M. Zhong, J. Han, and W. Wang, Reliability analysis of interdependent hypergraph network under different attack strategies, Int. J. Mod. Phys. C **34**, 2350027 (2023).

[57] H. Sun and G. Bianconi, Higher-order percolation processes on multiplex hypergraphs, Phys. Rev. E **104**, 034306 (2021).

[58] S. Boccaletti, P. De Lellis, C. del Genio, K. Alfaro-Bittner, R. Criado, S. Jalan, and M. Romance, The structure and dynamics of networks with higher order interactions, Phys. Rep. **1018**, 1 (2023).

[59] M. Newman, *Networks* (Oxford University Press, New York, 2018).

[60] I. Bonamassa, B. Gross, and S. Havlin, Interdependent couplings map to thermal, higher-order interactions, arXiv:2110.08907.

[61] S.-W. Son, G. Bizhani, C. Christensen, P. Grassberger, and M. Paczuski, Percolation theory on interdependent networks based on epidemic spreading, Europhys. Lett. **97**, 16006 (2012).